

Simultaneous removal of SO₂ and NO_x from flue gas using a CuO/Al₂O₃ catalyst sorbent

II. Promotion of SCR activity by SO₂ at high temperatures

Guoyong Xie, Zhenyu Liu,* Zhenping Zhu, Qingya Liu, Jun Ge, and Zhanggeng Huang

State Key Laboratory of Coal Conversion, Institute of Coal Chemistry, Chinese Academy of Sciences, Taiyuan, Shanxi 030001, People's Republic of China

Received 30 October 2003; revised 30 January 2004; accepted 10 February 2004

Abstract

Promoting effect of SO₂ on selective catalytic reduction (SCR) of NO by NH₃ over a CuO/Al₂O₃ catalyst sorbent has been investigated. Transient experiment, X-ray photoelectron spectroscopy (XPS), in situ DRIFT, NH₃-TPD, and temperature-programmed reduction (TPR) were used to evaluate the promoting mechanism. The results show that the presence of SO₂ in the reaction stream can significantly promote catalytic activity of NO reduction at temperatures above 300 °C due to the formation of sulfate species on the catalyst surface. Sulfate species affect SCR activity by changing the acidity and redox property of the catalyst sorbent. In situ DRIFT shows that only ammonia coordinated on Lewis acid sites is found on the CuO/Al₂O₃ catalyst sorbent. Sulfation of CuO/Al₂O₃ catalyst sorbent greatly increases the concentration and strength of Lewis acid sites and the concentration of Brønsted acid sites. However, the ammonia bound to Brønsted acid sites does not play an important role in the SCR reaction in the catalyst system. Moreover, there is a close relationship between the SCR activity and ammonia oxidation activity. Ammonia oxidation experiments and TPR in H₂ suggest that sulfation of the catalyst sorbent weakens the catalyst's oxidation ability and inhibits NH₃ oxidation to NO in the process of SCR, which may be another main promoting effect of SO₂ on SCR.

© 2004 Elsevier Inc. All rights reserved.

Keywords: SO₂; Promoting effect; NO_x; Selective catalytic reduction (SCR); Ammonia oxidation; CuO/Al₂O₃

1. Introduction

Simultaneous SO₂ and NO_x removal from stationary sources can be achieved with high efficiency using copper on alumina catalyst sorbents (CuO/Al₂O₃), which act both as catalysts for oxidation of SO₂ to SO₃ and as sorbents for SO₃ to form copper sulfate and aluminum sulfate and also catalyze the reduction of NO_x to N₂ in the presence of NH₃ and O₂ [1–3].

Many studies have been done on the catalyst sorbents, which reveal that SO₂ has a complicated effect on the SCR activity, deactivating the SCR activity at temperatures below 300 °C but promoting the SCR activity at temperatures greater than 350 °C [4–6]. However, few studies have been done on the detailed mechanism of this SO₂ effect.

Studies on many supported metal oxide SCR catalysts [7–10], other than CuO/Al₂O₃, show that the promoting effect of SO₂ is due to the formation of surface sulfate species, which increases the surface acidity of the catalysts and favors ammonia adsorption. However, it was also reported that ammonia oxidation to NO is the main reason for decreased SCR activity at high temperatures [11], so the promotion by SO₂ may also be associated with changes in ammonia oxidation activity due to changes in redox property of the catalyst; however, no literature was found in this regard. Attributions were also made to increases in both Brønsted acidity and Lewis acidity upon SO₂ adsorption, but which acid site is effective in the SCR reaction is still in debate [6,7,11,12]. At this stage, it is very interesting to study the promoting effect of SO₂ on CuO/Al₂O₃ catalyst sorbent at high temperatures, especially on changes in ammonia oxidation activity of the catalyst sorbent, which may bring a better understanding on the effect of SO₂ on this catalyst sorbent as well as other SCR catalysts.

* Corresponding author. Fax: +86-351-4050320.
E-mail address: zyl@public.ty.sx.cn (Z. Liu).

In this paper, a comprehensive study is made to understand the effect of SO₂ on SCR of NO during simultaneous removal of SO₂ and NO_x using fresh and sulfated CuO/Al₂O₃ catalyst sorbents at temperatures greater than 300 °C through evaluations on surface acidity, ammonia oxidation activity, and redox property of the catalyst sorbents.

2. Experimental

2.1. Preparation and physicochemical analysis of the catalyst sorbent

The CuO/Al₂O₃ catalyst sorbent was prepared by pore volume impregnation of pure γ -Al₂O₃ pellets (30–40 mesh, BET surface area of 185 m² g⁻¹, Fushun Petrochemical Co.) with an aqueous solution of copper(II) nitrate, as described in detail elsewhere [13]. After the impregnation, the catalyst sorbent was dried at 50 °C for 8 h and 120 °C for 5 h and then calcined in air at 400 °C for 8 h.

The calcined catalyst sorbent contains 8.0 wt% Cu as confirmed by ICP analysis and is termed Cu8 in the text. The Cu8 shows a BET surface area of 149 m² g⁻¹ and no crystalline materials in X-ray diffraction except the alumina support.

2.2. Activity measurements

SCR activity of Cu8 and sulfated Cu8 was measured in a fixed-bed quartz reactor (16 mm i.d.). The experimental equipment consists of three sections: a reactor, a gas feeding system, and a gas analyzer. 2.0 g of sample was placed between two plugs of quartz wool held in the reactor, which was heated by a vertical electrical furnace. A thermocouple was inserted inside the reactor for actual temperature measurement. The feed contained 620 ppm NO, 620 ppm NH₃, 1600 ppm SO₂ (when used), 3 vol% H₂O, 5.5 vol% O₂, and balance Ar. In all the runs, the total flow rate was controlled at 460 ml min⁻¹, which corresponds to a space velocity (GHSV) of 14000 L kg h⁻¹. H₂O was introduced to the reactor by passing the Ar and O₂/Ar streams through a heated gas-wash bottle containing deionized water. The concentrations of NO, NO₂, SO₂, and O₂ at the inlet and outlet of the reactor were monitored by an on-line flue gas analyzer (KM9006 Quintox, Kane international Limited) equipped with NO, NO₂, SO₂, and O₂ sensors.

Sulfated Cu8 was made from sulfation of Cu8 at 400 °C in a stream containing 1600 ppm SO₂, 3 vol% H₂O, 5.5 vol% O₂, and balance Ar. To acquire sulfated Cu8 of different sulfur contents, the sulfation experiments were performed in different times on stream, yielding samples with sulfur contents of about 0.3, 0.6, 1.2, 2.4, and 6.0 wt%, which are termed S0.3-Cu8, S0.6-Cu8, S1.2-Cu8, and S2.4-Cu8, S6.0-Cu8, respectively.

2.3. Oxidation of ammonia

The ammonia oxidation experiments were performed in the same reactor with 2.0 g of Cu8 or S6.0-Cu8. The feed contained 1000 ppm NH₃, 5 vol% O₂, and balance Ar. The total flow rate was 460 ml min⁻¹ at ambient conditions. The product stream was monitored on-line by a mass-quadrupole detector (Blazers, OmniStar 200) for NH₃ ($m/e = 17$ minus the contribution of H₂O), H₂O ($m/e = 18$), N₂ ($m/e = 28$), NO ($m/e = 30$), O₂ ($m/e = 32$), N₂O ($m/e = 44$), and NO₂ ($m/e = 46$).

2.4. X-ray photoelectron spectroscopy (XPS)

XPS measurements were carried out at room temperature on a VG-Scientific Escalab 220 I-XL. The binding energies were calculated with respect to the C 1s peak set at 284.6 eV.

2.5. In situ DRIFT experiments

DRIFT spectra were recorded on a Bruker Equinox55 FTIR instrument equipped with a diffuse reflectance cell and a controlled environmental chamber (Spectra-Tech, 0030-102) equipped with ZnSe windows. The samples were ground into powder and mounted on a ceramic frit (Al₂O₃), which could be heated to elevated temperatures via a PID controller. Ar (purity 99.999%, dried over a 5A zeolite cartridge), synthetic air (10% O₂ purity 99.999%, 90% Ar purity 99.999%, dried over a 5A zeolite cartridge), and ammonia (3600 ppm in argon, dried over a KOH cartridge) were controlled by mass flowmeters. The DRIFT spectra in the reflection mode were taken by accumulating 100 scans at a resolution of 4 cm⁻¹ and transformed to the Kubelka–Munk function. Prior to all experiments, the samples were activated in the synthetic air stream (50 ml min⁻¹) at 400 °C for 2 h to oxidize and remove impurities on the surface of the catalyst sorbents. The samples were then cooled down to room temperature at a rate of 6 °C min⁻¹, and spectra were collected at every 30 °C as background spectra. Ammonia was adsorbed at room temperature. Thereafter, the cell was flushed with Ar (50 ml min⁻¹) for 2 h. Temperature-programmed desorption of ammonia (NH₃-TPD) was performed at a rate of 6 °C min⁻¹, and spectra were collected at every 30 °C. The final spectra were obtained by subtracting the corresponding background spectra. During NH₃-TPD, the product stream was monitored on-line by the mass-quadrupole detector (Blazers, OmniStar 200).

3. Results and discussion

3.1. Effect of SO₂ on SCR activity

When fresh Cu8 is exposed to flue gas (containing SO₂, NO_x, O₂, etc.), a sulfation reaction takes place, which converts CuO in Cu8 to CuSO₄. The effect of reaction temperature on SCR activities (expressed as a fraction of NO

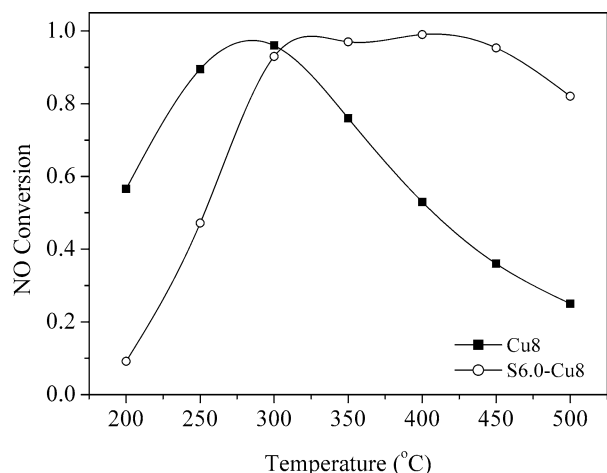


Fig. 1. Effects of SO_2 on the SCR activity of Cu8 catalyst sorbent as a function of temperature. Experimental conditions: 620 ppm NO, 620 ppm NH_3 , 5.5 vol% O_2 , 3 vol% H_2O , GHSV of $14000 \text{ L kg}^{-1} \text{ h}^{-1}$.

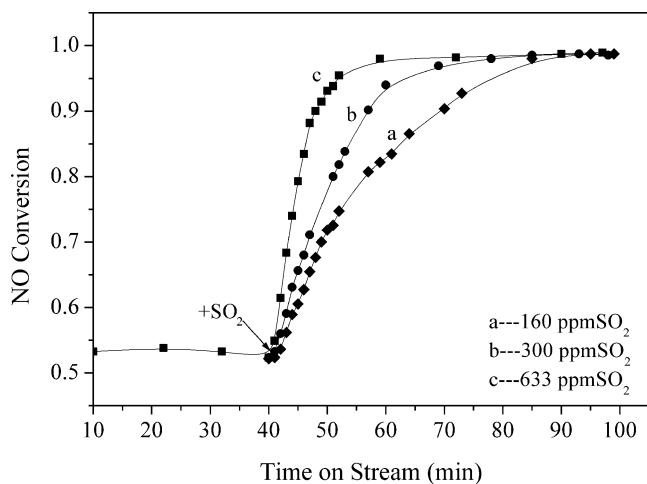


Fig. 2. Dependence of NO conversion on Cu8 surface sulfation with different SO_2 concentration. Experimental conditions: 620 ppm NO, 620 ppm NH_3 , 5.5 vol% O_2 , 3 vol% H_2O , 160–633 ppm SO_2 , 400°C , GHSV of $14000 \text{ L kg}^{-1} \text{ h}^{-1}$.

conversion at steady state) of Cu8 and S6.0-Cu8 (contains 6.0 wt% sulfur) are shown in Fig. 1. NO conversions exhibit maximum values with variation of reaction temperature over both catalyst sorbents. For S6.0-Cu8, the NO conversions are greater than 95% in the temperature of 300–450°C. This range is 100°C higher and much wider than that for Cu8. The decrease in NO conversion at high temperatures may result from increased NH_3 oxidation [11], which not only causes a decrease in surface ammonia concentration for the SCR reaction but also produces more NO. Fig. 1 suggests that SO_2 inhibits the SCR activity of the Cu8 catalyst sorbent at temperatures of 200–300°C, whereas it shows promoting effect at temperatures greater than 300°C.

Transient experiment is used to illustrate the relationship between SCR activity and the extent of sulfation beyond 300°C. Fig. 2 shows the responses in NO conversion upon introduction of SO_2 of different concentrations at 400°C. It

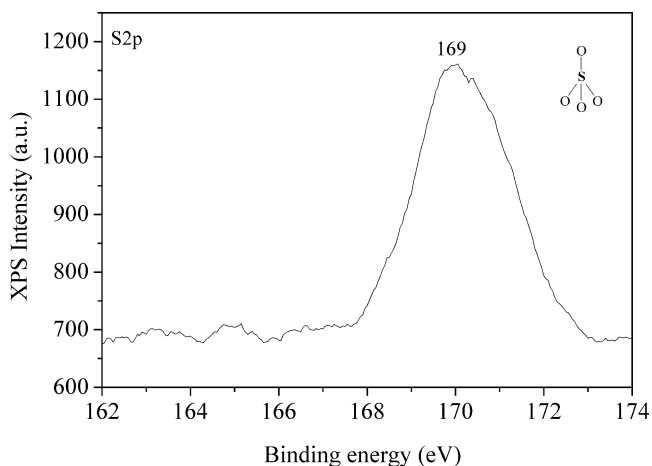


Fig. 3. XPS spectrum of S $2p$ for S6.0-Cu8 catalyst sorbent.

should be pointed out that there is no SO_2 in the feed in the first 40 min. The NO conversions show a fast increase upon SO_2 introduction and the increase is faster at higher SO_2 concentrations than that at lower SO_2 concentration. Since the rate of catalyst sorbent sulfation depends on SO_2 concentration, this result indicates that the SCR activity is closely related to the extent of catalyst sorbent sulfation. It is interesting to note that when the NO conversion reaches the same stable level of about 98% at time on stream of about 95, 78, and 59 min for curves a, b, and c in Fig. 2, the sulfur content of the catalyst sorbent is about 0.3 wt% (through integration of SO_2 conversion curves, determined by the difference between the inlet and the outlet SO_2 concentrations of the reactor, with time on stream). This suggests that a sulfur content of 0.3 wt% is needed for stable and high SCR activity over the catalyst sorbent.

3.2. Characterization of sulfates

3.2.1. XPS characterization

XPS was used to characterize chemical morphology of sulfur in sulfated Cu8 catalyst sorbent. As shown in Fig. 3, S6.0-Cu8 exhibits a S $2p$ peak at about 169 eV, corresponding to sulfur in the sulfate form [13,14], which indicates formation of sulfate species during the interaction of Cu8 with SO_2/O_2 .

3.2.2. DRIFT characterization

Sulfates, sulfites, and adsorbed sulfur oxide species show vibration bands in $1500\text{--}600 \text{ cm}^{-1}$ infrared region, and thus infrared characterization is used to identify the species formed during the interaction of SO_2/O_2 with the $\text{CuO}/\text{Al}_2\text{O}_3$ catalyst sorbents. The DRIFT spectrum of S6.0-Cu8 is shown in Fig. 4. Due to the strong absorption of skeletal vibrations of the alumina support for frequencies below 1000 cm^{-1} , the absorption in the range of $1000\text{--}1600 \text{ cm}^{-1}$ is only analyzed. Gauss fitting of the spectrum shows three main bands at 1248, 1188, and 1104 cm^{-1} and two weak shoulders at 1364 and 1313 cm^{-1} , which may be

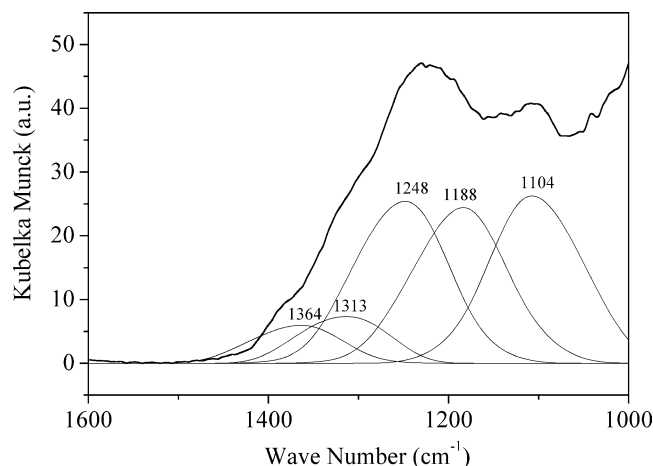


Fig. 4. DRIFT spectrum of S6.0-Cu8 catalyst sorbent.

attributed to sulfate species. These are similar to but with noticeable differences from those reported by Centi [15] and Waqif [16] for a sulfated CuO/Al₂O₃ catalyst sorbent. The differences are in relative intensities and small shifts in peak positions. Infrared spectra of sulfated metal oxides generally show absorption bands at 1390–1360 cm⁻¹ and broad bands at 1250–900 cm⁻¹. The peak in 1390–1360 cm⁻¹ is from stretching frequency of S=O and the peaks in 1250–900 cm⁻¹ are the characteristic of SO₄²⁻ due to lowering of the symmetry in the free SO₄²⁻ (Td point) [17]. According to Waqif [16], these different sulfate species on the CuO/Al₂O₃ catalyst sorbent include sulfate species on Al₂O₃ with $\nu(\text{S}=\text{O})$ bands at 1364 cm⁻¹ and species in interaction with Cu²⁺ or with Cu²⁺ and Al³⁺ with broad adsorption bands from 1250 to 1040 cm⁻¹.

3.3. Acidity characterization

Surface acidity that favors ammonia adsorption is an important factor in SCR reaction. The strong ability of S=O in sulfate complexes to accommodate electrons from a basic molecule is a driving force in the generation of highly acidic properties [18,19]. Accordingly, to investigate the effect of sulfate species on the acidity, in situ DRIFT and TPD experiments were carried out.

Ammonia is often used as a basic probe molecule in infrared spectroscopy to characterize acid sites in catalysts. Besides this, ammonia itself is a reactant of the SCR reaction and the adsorbed ammonia species play a predominant role in the reaction mechanism [20]. Hence, ammonia adsorption was studied to gain information about the surface acidity of Cu8 and sulfated Cu8s of different sulfur contents (shown in Fig. 5). After Cu8 is treated in a flow of 3600 ppm NH₃/Ar at room temperature for 30 min and then purged with Ar for 2 h at room temperature, a strong band at 1625 cm⁻¹ and weaker bands at 3390, 3223, and 3180 cm⁻¹ are observed (Fig. 5a). The band at 3390 cm⁻¹ is due to the asymmetric stretching vibration frequency of coordinated NH₃ [11]. The band at 3223 and 3180 cm⁻¹ is in accordance with the liter-

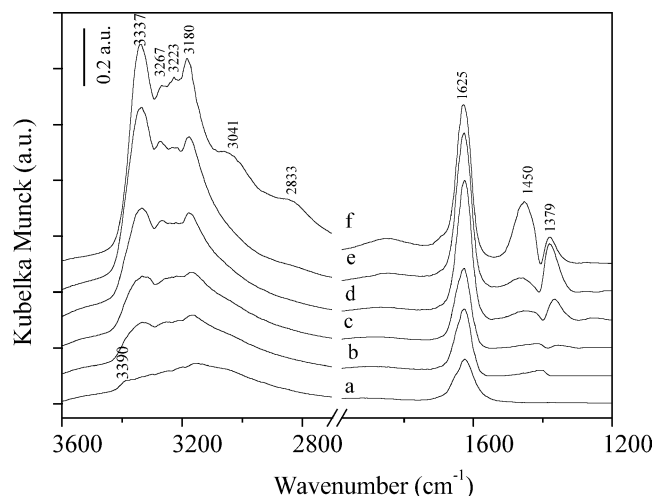


Fig. 5. In situ DRIFTS spectra of ammonia adsorption at room temperature over (a) Cu8, (b) S0.3-Cu8, (c) S0.6-Cu8, (d) S1.2-Cu8, (e) S2.4-Cu8, and (f) S6.0-Cu8.

ature [21] and assigned to the split due to Fermi resonance with the overtone of the asymmetric NH₃ deformation. In the N–H bending region, the band at 1625 cm⁻¹ is assigned to the asymmetric bending vibrations of coordinated NH₃. These results indicate that ammonia adsorbed on the Cu8 catalyst sorbent is mainly in the form of coordinated ammonia, and the CuO/Al₂O₃ catalyst sorbent is Lewis acidic.

Intensity of the above-coordinated ammonia bands increase with increasing sulfur content of sulfated Cu8 (Fig. 5b–5f), and the band at 3390 cm⁻¹ is shifted to 3337 cm⁻¹, suggesting increased strength and concentration of Lewis acid sites from sulfating the catalyst sorbent. When sulfur content in sulfated Cu8 reaches 1.2 wt% (Fig. 5d), new bands at 3267, 1450, and 1379 cm⁻¹ are detected. With further increase in sulfur content to 6.0 wt% (Fig. 5f), additional new bands at 3041 and 2833 cm⁻¹ are observed. The adsorbed bands at 3267, 3041, and 2833 cm⁻¹ are due to the stretching vibration of NH₄⁺ species bound to Brønsted acid sites. The band at 1450 cm⁻¹ is assigned to the asymmetric bending vibration of NH₄⁺ [22,23]. The band at 1379 cm⁻¹ may arise from changes in the sulfate spectrum induced by the adsorption of ammonia [10]. These results suggest that the increasing sulfate content in CuO/Al₂O₃ catalyst sorbent not only strengthens Lewis acidity but also produces new Brønsted acid sites.

From the aforementioned results, it seems interesting to further identify the nature of the acid sites, Lewis or Brønsted, which is the active site for ammonia activation. On Cu8 and sulfated Cu8 with sulfur contents of 0.3 and 0.6 wt% (Fig. 5a–5c), no ammonium ions bound to Brønsted acid sites were observed, indicating that the active site is not Brønsted acidic, which agrees with that reported for pure Al₂O₃ support [24] and for pure CuO [25]. Since these samples indeed show high SCR activity, it may suggest that Lewis acid sites are responsible for ammonia activation, and the existence of Brønsted acidity is not a requisite

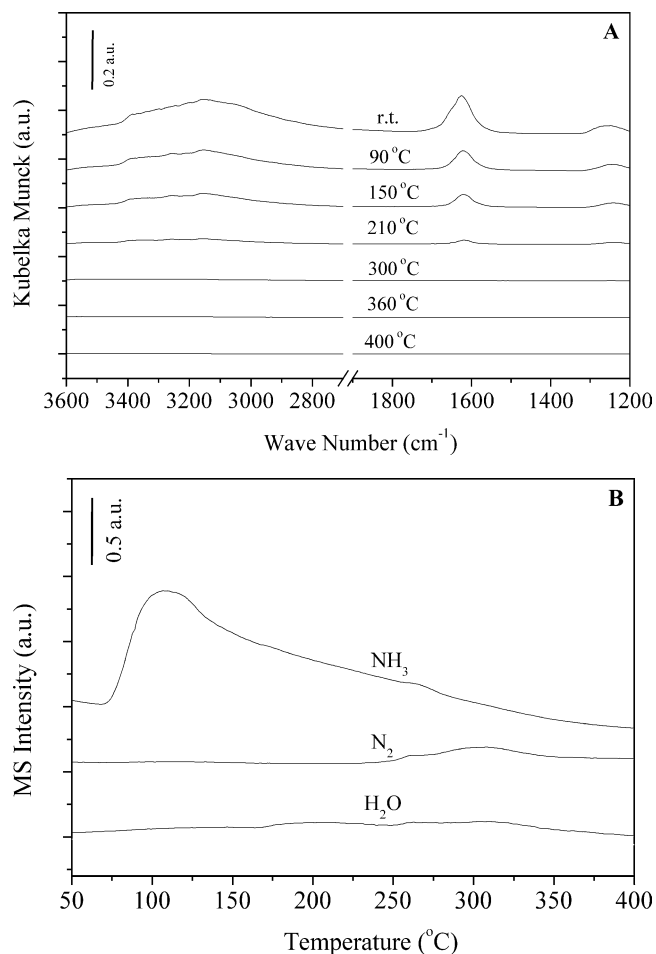


Fig. 6. TPD of ammonia from Cu8 at a heating of $6\text{ }^{\circ}\text{C min}^{-1}$. (A) DRIFT spectra at different temperatures; (B) corresponding mass spectrum.

for the SCR reaction on Cu8. Other catalysts where Brønsted acidity is absent or very weak, such as CuO/TiO₂ [11], MnOx/TiO₂ [31], Fe₂O₃/TiO₂ [30], and Fe₂O₃ [11,31], are also active for SCR reaction.

TPD of Cu8 and S6.0-Cu8 pre-adsorbed with ammonia was performed from room temperature to 400 °C in Ar at a rate of $6\text{ }^{\circ}\text{C min}^{-1}$ (Figs. 6 and 7). As shown in Fig. 6A for Cu8, bands of ammonia adsorption on Cu8 decrease to disappear at temperatures below 300 °C. The corresponding mass spectra of desorbed species, in Fig. 6B, show that ammonia exhibits a maximum desorption rate at about 120 °C, with a gradual tailing toward higher temperatures. Trace amounts of nitrogen and water were observed at above 250 °C, which may result from oxidation of adsorbed ammonia by lattice oxygen. Other oxidation products such as N₂O, NO, or NO₂ were not detected. This behavior was also observed on a variety of other SCR catalysts [26].

For S6.0-Cu8 catalyst sorbent, Fig. 7, the ammonia bound to Lewis acid sites (3337, 3180, and 1625) decrease gradually with increasing temperature, and sharp decreases were observed above 300 °C. At 400 °C, little of Lewis-bound ammonia species remain. Instead of the slow, continuous de-

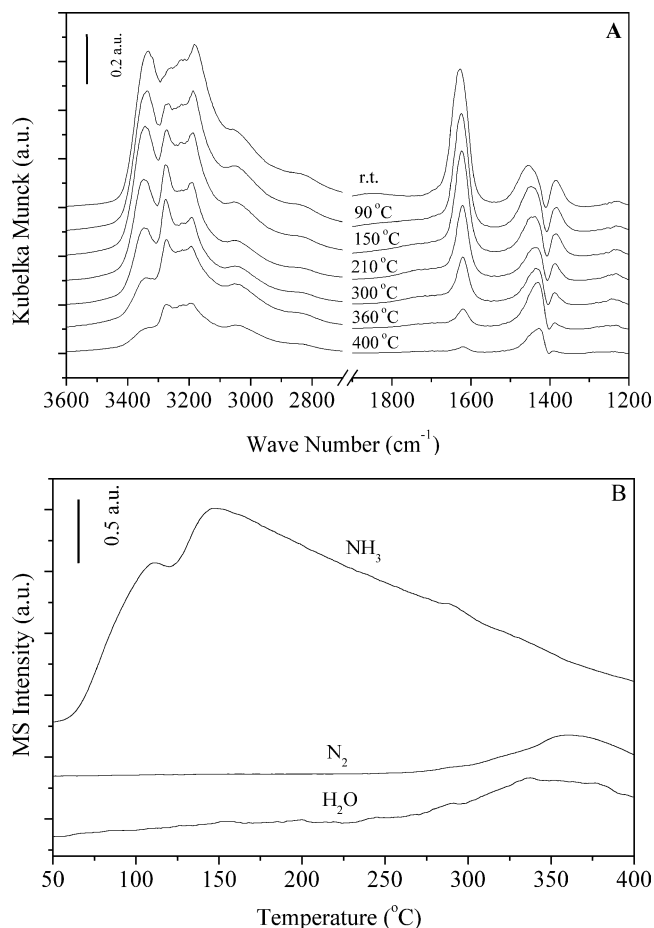


Fig. 7. TPD of ammonia from S6.0-Cu8 at a heating of $6\text{ }^{\circ}\text{C min}^{-1}$. (A) DRIFT spectra at different temperatures; (B) corresponding mass spectrum.

crease in the intensity of the coordinated ammonia, there is a slight enhancement in intensity of NH₄⁺ bands (Brønsted acid sites, 3041, 2883, and 1450 cm⁻¹) from room temperature up to 90 °C, which may result from protonation of the Lewis-bound ammonia. After this initial increase, the intensity of the band keeps almost constant until about 360 °C. At 400 °C, quite a bit of ammonium ions on Brønsted acid sites are still observable. The initial increase in NH₄⁺ band intensity is accompanied by a downward frequency shift of the NH₄⁺ band from 1450 cm⁻¹ at room temperature to 1429 cm⁻¹ at above 150 °C, indicating the presence of sites of different acidity on the catalyst sorbent. A correlation of the band position with the acidity of the metal center was also found by Nakamoto for amine complexes [17]. The above results suggest that the Brønsted-bound ammonium ions are thermally more stable than the Lewis-bound molecular ammonia species, which is consistent with results of Long et al. [27], but is contradictory to the results of Rajadhayaksha et al. [28]. The corresponding mass spectra of desorbed species from S6.0-Cu8, Fig. 7B, show continued release of ammonia over a wide temperature range, suggesting the presence of a broad distribution of ammonia adsorp-

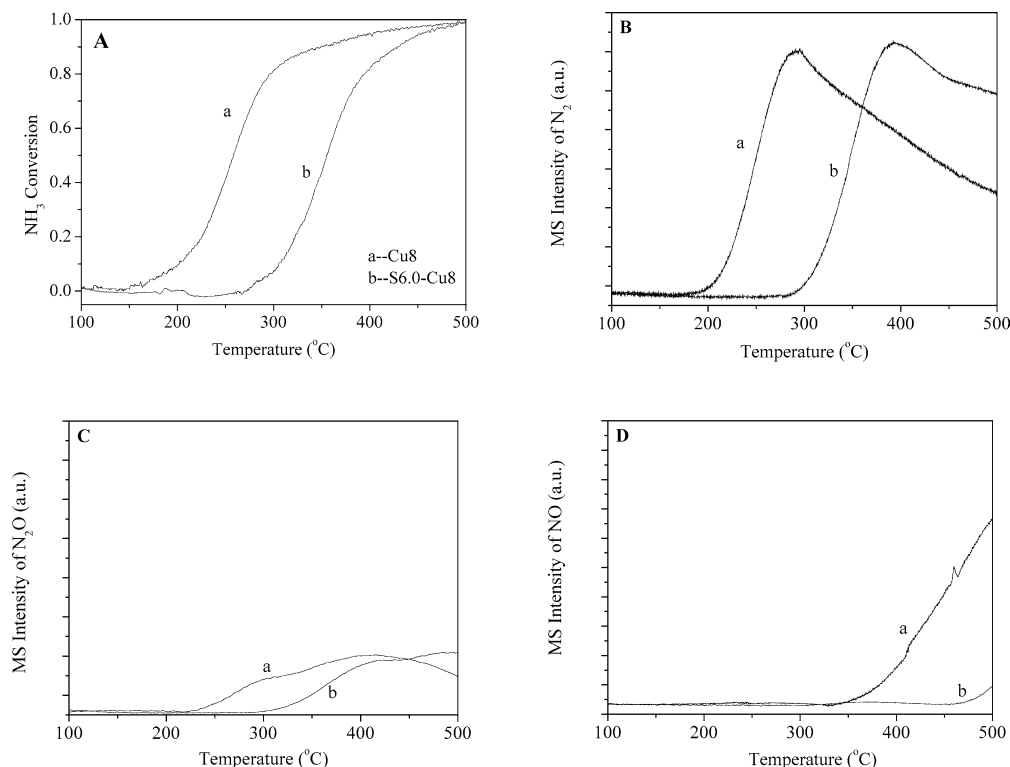


Fig. 8. NH₃ oxidation on (a) Cu8 and (b) S6.0-Cu8 as a function of temperature. (A) NH₃ conversion; (B) N₂ formation; (C) N₂O formation; (D) NO formation.

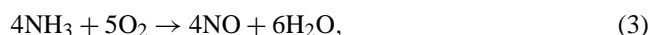
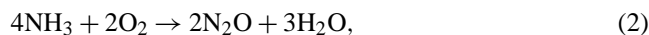
tion sites. The oxidation of ammonia by lattice oxygen during ammonia TPD also occurred as evidenced by the desorption of water and nitrogen at high temperatures, which may account for the sharp decrease in DRIFT bands for Lewis-bound ammonia at above 300 °C, whereas the Brønsted bound ammonium ions are stable from oxidation, which further supports the suggestion that Brønsted acid sites are not necessary for SCR reaction. The results of TPD of ammonia also indicate that the concentration of acid sites (total amount of ammonia desorbed, including those oxidized to form nitrogen) and their strength (temperature for complete ammonia desorption) were greatly enhanced by sulfation as characterized with DRIFT, which may be a reason for high NO conversion over sulfated catalyst sorbent at high temperatures.

3.4. NH₃ oxidation

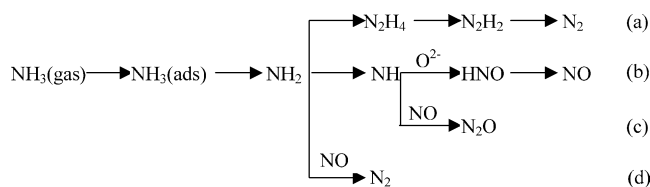
During the SCR reaction, the reaction of NH₃ with NO + O₂ and that with O₂ are known as two competitive reactions. Inhibition of NH₃ + O₂ (direct NH₃ oxidation) and enhancement of NH₃ + NO + O₂ will both be beneficial to NO reduction. In fact, direct ammonia oxidation may be the main reason for decreased SCR activity at high temperature. It is important, therefore, to evaluate the activity of NH₃ oxidation on Cu8 and sulfated Cu8. Variations in NH₃ conversion and formation of N₂, N₂O, and NO during NH₃ oxidation as functions of temperature are presented in Figs. 8A–8D, respectively. As shown in Fig. 8A, Cu8 and S6.0-Cu8 are

active in ammonia oxidation in different temperature ranges. Cu8 shows an NH₃ conversion of 90% at about 330 °C, while S6.0-Cu8 shows at about 430 °C. These results are in general agreement with the literature that shows that copper-containing catalysts are active in oxidation reactions [29].

In Fig. 8B, N₂ formed in ammonia oxidation increases with temperature and reaches a maximum at about 290 °C for Cu8 and 390 °C for S6.0-Cu8. The formation of N₂O (Fig. 8C) is similar to that of N₂ initially, but shows a second peak at high temperature. The evolutions of NO (Fig. 8D) start at temperatures higher than that of N₂ and N₂O. These indicate that the ammonia is mainly oxidized to N₂ and N₂O at low temperatures possibly following Eqs. (1) and (2) and to NO at high temperatures possibly following Eqs. (3) and (4),



It is important to note that the initial temperature of NH₃ oxidation on S6.0-Cu8 is about 100 °C higher than that on Cu8, so does the formation of N₂, N₂O, and NO during NH₃ oxidation. This suggests that S6.0-Cu8 is less active for NH₃ oxidation than Cu8, and which may be a factor on the promoting effect of SO₂ on SCR of NO at high temperatures. This phenomenon seems to not result from strong ammonia adsorption ability of S6.0-Cu8 because it affects both SCR



Scheme 1. Possible reaction scheme for NH_3 oxidation (a, b, c) and SCR of NO (d) [11,30].

and NH_3 oxidation reactions. Hence, it is likely that the sulfation may change the redox property of the catalyst sorbent, which affects the oxidation ability of the catalyst sorbent and then the SCR activity. The study on H_2 -TPR of Cu8 and sulfated Cu8 in part I of this series points to a major decrease in oxidation ability of the $\text{CuO}/\text{Al}_2\text{O}_3$ catalyst sorbent by sulfation, indicating reduced reactivity of lattice oxygen in sulfated Cu8 with the reducing agent (H_2) compared to Cu8. It should be noted that the oxidation ability of the catalyst sorbent influences the activation of ammonia, and the difference in oxidation ability between Cu8 and sulfated Cu8 can be directly related to the difference in activity of ammonia oxidation.

The relation between the activity in NH_3 oxidation and in SCR for Cu8 and S6.0-Cu8 (as shown in Fig. 8 and 1) suggests that these two reactions possibly follow similar mechanism. The mechanism shown in Scheme 1 is proposed for copper- and iron-containing catalysts [11,30], which suggests that NH_2 is the common intermediate for both NH_3 oxidation and SCR. If this holds for Cu8 and sulfated Cu8, the SCR reaction is in competition with ammonia oxidation through the intermediate amide NH_2 . In the absence of NO, only NH_3 oxidation occurs that results in the formation of N_2 at low temperatures (a) and N_2O and NO at high temperatures (b, c). In the presence of NO, both NH_3 oxidation and SCR of NO (d) occur. A good SCR catalyst is the one which promotes the reaction d and inhibits reactions a, b, and c. Clearly, this is the case for sulfated Cu8 catalysts.

Based on this scheme, the data in this paper seem to suggest that the higher SCR activity of Cu8 than that of sulfated Cu8 at low temperature results from the stronger oxidation ability of Cu8 than that of sulfated Cu8. However, at high temperatures, the stronger oxidation ability of Cu8 makes the subsequent hydrogen abstraction from NH_2 easier, which increases the NH_3 oxidation reaction for NO and decreases the SCR reaction for removal of NO. But the sulfation, to form sulfated Cu8, weakens catalyst's oxidation ability and inhibits deep oxidation of NH_3 , which results in increase in SCR of NO.

4. Conclusion

SO_2 shows the promoting effect on SCR activity over the $\text{CuO}/\text{Al}_2\text{O}_3$ catalyst sorbent above 300°C due to the formation of sulfate species on the catalyst sorbent surface. The promoting effect of sulfate species can be attributed not only

to increased acidity of the catalyst sorbent, which favors adsorption of ammonia for SCR reaction, but also to decreased oxidation ability of the catalyst sorbent's and reduced NH_3 oxidation activity. The presence of NH_3 adsorbed on Brønsted acid sites is not necessary for the SCR reaction to take place.

The very different SO_2 effects, deactivation or promotion, on SCR activity of $\text{CuO}/\text{Al}_2\text{O}_3$ catalyst sorbent at different temperatures may result mainly from the same phenomenon: the formation of sulfate salts on the surface. The difference can be attributed to the changes in SCR activities of the sulfates at different temperatures. At temperatures below 300°C , the sulfates are not active enough for SCR of NO, which results in accumulation of ammonium sulfates on the surface and then further decrease of SCR activity. At temperatures greater than 300°C , the SCR activities of the sulfates are high, which limits the accumulation of ammonium sulfates.

Acknowledgments

The authors gratefully acknowledge the financial support from the Natural Science Foundation of China (20276078, 90210034), the National High-Tech Research and Development Program (the 863 Program, 2002AA529110), Chinese Academy of Sciences, and the Shanxi Natural Science Foundation.

References

- [1] G. Centi, A. Riva, N. Passarini, G. Brambilla, B.K. Hodnett, *Chem. Eng. Sci.* 45 (1990) 2679.
- [2] J.N. Armor, *Appl. Catal. B* 1 (1992) 221.
- [3] C. Macken, B.K. Hodnett, G. Paparatto, *Ind. Eng. Chem. Res.* 39 (2000) 3868.
- [4] G. Centi, N. Passarini, S. Perathoner, A. Riva, *Ind. Eng. Chem. Res.* 31 (1992) 1963.
- [5] S.M. Jeong, S.H. Jung, K.S. Yoo, S.D. Kim, *Ind. Eng. Chem. Res.* 38 (1999) 2210.
- [6] S.M. Jeong, S.D. Kim, *Ind. Eng. Chem. Res.* 39 (2000) 1911.
- [7] J.P. Chen, R.T. Yang, *J. Catal.* 139 (1993) 277.
- [8] S.M. Jung, P. Grange, *Appl. Catal. B* 27 (2000) L11.
- [9] Z. Zhu, Z. Liu, H. Niu, S. Liu, *J. Catal.* 187 (1999) 245.
- [10] D. Pietrogiamomi, D. Sannino, A. Magliano, P. Ciambelli, S. Tuti, V. Indovina, *Appl. Catal. B* 36 (2002) 217.
- [11] G. Ramis, L. Yi, G. Busca, M. Turco, E. Kotur, R.J. Willey, *J. Catal.* 157 (1995) 523.
- [12] R.Q. Long, R.T. Yang, *Appl. Catal. B* 33 (2001) 97.
- [13] G. Xie, Z. Liu, Z. Zhu, Q. Liu, J. Ma, *Appl. Catal. B* 45 (2003) 213.
- [14] C.H. Wang, C.N. Lee, H.S. Weng, *Ind. Eng. Chem. Res.* 37 (1998) 1774.
- [15] G. Centi, N. Passarini, S. Perathoner, A. Riva, *Ind. Eng. Chem. Res.* 31 (1992) 1963.
- [16] M. Waqif, O. Saur, J.C. Lavalley, *J. Phys. Chem.* 95 (1991) 4051.
- [17] K. Nakamoto, *Infrared and Raman Spectra of Inorganic and Coordination Compounds*, fourth ed., Wiley, New York, 1986.
- [18] R.J. Gillespie, E.A. Robinson, *Can. J. Chem.* 41 (1963) 2074.
- [19] T. Yamaguchi, T. Jin, K. Tanabe, *J. Phys. Chem.* 90 (1986) 3148.
- [20] G. Busca, L. Lietti, G. Ramis, F. Berti, *Appl. Catal. B* 18 (1998) 1.

- [21] G. Busca, *Langmuir* 2 (1986) 577.
- [22] R.Q. Long, R.T. Yang, *J. Catal.* 186 (1999) 254.
- [23] N.-Y. Topsøe, H. Topsøe, J.A. Dumesic, *J. Catal.* 151 (1995) 226.
- [24] R. Fledorow, I.G. Dalla Lana, *J. Phys. Chem.* 84 (1980) 2779.
- [25] G. Busca, *J. Mol. Catal.* 43 (1987) 225.
- [26] H. Schneider, S. Tschudin, M. Schneider, A. Wokaun, A. Baiker, *J. Catal.* 147 (1994) 5.
- [27] R.Q. Long, R.T. Yang, *J. Catal.* 194 (2000) 80.
- [28] R.A. Rajadhyaksha, H. Knozinger, *Appl. Catal.* 51 (1989) 81.
- [29] A. Wöllner, F. Lange, H. Schmelz, H. Knözinger, *Appl. Catal. A* 94 (1993) 181.
- [30] J.M.G. Amores, V.S. Escibano, G. Ramis, G. Busca, *Appl. Catal. B* 13 (1997) 45.
- [31] V. Lorenzelli, G. Busca, *Mater. Chem. Phys.* 13 (1985) 261.